

The effect of a steady drift on the dispersion of a particle in turbulent fluid

By A. NIR AND L. M. PISMEN

Department of Chemical Engineering, Technion-Israel Institute of Technology,
Haifa, Israel

(Received 21 March 1978 and in revised form 11 September 1978)

The effect of a steady deterministic drift on the dispersion of particles suspended in a stationary homogeneous turbulent field is examined using previously reported closed equations of the mean-squared particle displacement. The existence of negative particle velocity correlations is demonstrated. The dependence of the particle diffusivity and kinetic energy on the inertia and drift factors is evaluated for a model turbulence spectrum. Asymptotic formulae are obtained for the case of dominant deterministic motion. The theory is applied to analysis of the experimental data of Snyder & Lumley (1971), and good and consistent agreement with these asymptotic formulae was obtained after accounting for the quasi-stationarity of particle velocity correlation functions in decaying turbulence.

1. Introduction

In a recent communication (Pismen & Nir 1978 – henceforth referred to as I) we have considered the problem of particle motion in a stationary homogeneous turbulent field. The closed equation for the mean-squared displacement of the particle, R_{ij} , was derived using the independence approximation (Corrsin 1959) and the Gaussian property of the turbulent velocity field. The main steps of the derivation are described below.

Consider a particle obeying a linear interaction law

$$\frac{dv_i}{dt} = \gamma(u_i - v_i), \quad (1)$$

where γ^{-1} is a scalar time constant and u_i and v_i are the random components of the fluid and particle velocities respectively. Equation (1) can also be written in the integral form

$$v_i = \gamma \int_0^t e^{-\gamma(t-t')} u_i(\mathbf{r}(t'), t') dt', \quad (2)$$

with

$$r_i(t) = \rho_i(t) + V_i t$$

denoting the particle trajectory. $\rho_i(t)$ is the random part of the particle displacement, with zero mean, while V_i represents a steady deterministic part of the particle velocity, relative to the fluid, owing to an external body force.

Using (2) we obtain the Lagrangian particle velocity correlation tensor

$$H_{ij}(t) = \lim_{\tau \rightarrow \infty} \langle v_i(\tau) v_j(\tau + t) \rangle = \frac{1}{2} \int_{-\infty}^{\infty} e^{-\gamma|t-t'|} \langle u_i(0, 0) u_j(\mathbf{r}(t'), t') \rangle dt', \quad (3)$$

which is evidently connected with the fluid velocity correlation tensor

$$G_{ij}(\mathbf{r}(t), t) = \langle u_i(0, 0) u_j(\boldsymbol{\rho}(t) + \mathbf{V}t, t) \rangle$$

at points lying on a particle trajectory. The angle brackets denote an ensemble average. In the particular cases when the random velocity component of the particle is negligible, i.e. $\gamma \rightarrow 0$ or $|\mathbf{V}| \gg |\mathbf{v}|$, G_{ij} reduces to the Eulerian correlation function at points lying on the particle's deterministic trajectory $V_i t$. This point will be used in the asymptotic analysis of § 3.

With a Fourier transform of the fluid velocity $G_{ij}(t)$ has the form

$$G_{ij} = \iint_{-\infty}^{\infty} \langle \tilde{u}_i(\mathbf{k}, 0) \tilde{u}_j(\mathbf{k}', t) \exp[-i\mathbf{k}' \cdot \boldsymbol{\rho}(t)] \rangle \exp[-i\mathbf{k}' \cdot \mathbf{V}t] d^3\mathbf{k}' d^3\mathbf{k}, \quad (4)$$

where $\tilde{u}_i(\mathbf{k}, t)$ is a spectral component. An implementation of Corrsin's (1959) conjecture and the Gaussian character of the velocity field enables a reduction of (3) and (4) to a closed equation connecting the particle mean-squared displacement tensor, $R_{ij}(t) = \langle \rho_i(t) \rho_j(t) \rangle$, with measurable Eulerian correlations of the turbulent fluid. (See I for a detailed derivation.) Thus

$$\frac{d^2 R_{ij}}{dt^2} = 2H_{ij}^{(s)} = \gamma \int_{-\infty}^{\infty} e^{-\gamma|t-t'|} dt' \int_{-\infty}^{\infty} \cos(\mathbf{k} \cdot \mathbf{V}t') \Phi_{ij}^{(s)}(\mathbf{k}, t') \exp[-\frac{1}{2}\mathbf{k}\mathbf{k} : \mathbf{R}(t')] d^3\mathbf{k}, \quad (5)$$

where Φ_{ij} is the turbulence spectral density and (s) denotes the symmetric part.

At $\gamma \rightarrow \infty$ and $\mathbf{V} = 0$, i.e. when the particle follows all turbulent pulsations, (5) coincides with Lundgren & Pointin's (1976) equation of the displacement of a fluid element.

The characteristics of random particle motion in an isotropic turbulent field, in the absence of an external body force, were calculated in detail in I. This case offers the best opportunity for analysing the influence of particle inertia in its pure form, free from interference of a superimposed deterministic motion. However, in practical situations the latter cannot be ignored and often plays a decisive role in determining the particle dispersion. This source of anisotropy is always present in experimental studies where the particle attains a steady terminal sedimentation velocity due to gravity.

Yudine (1959) and Csanady (1963) introduced the notion of 'crossing trajectories' to describe a deterministic gravitational drift, drawing the particle out of the strongly correlated fluid environment and thereby reducing the particle diffusivity. This effect is quantitatively described by (5) inasmuch as the oscillations of the cosine function effectively cut off correlations of the turbulent velocity field at times exceeding the characteristic time scale associated with the deterministic motion.

It is the purpose of this paper to apply the general approach presented in I to a non-isotropic system and to analyse the influence of the deterministic motion due to external body forces on the random displacement and kinetic energy of a suspended particle. A different procedure equivalent to consecutive iterations of (5) was recently used by Reeks (1977) as an extension of Phythian's (1975) analysis of turbulent self-diffusion.

Although the basic equation (5) cannot be reduced in this case to the scalar form studied in I, the presence of a deterministic drift brings certain theoretical advantages since it improves the closure approximation by reducing the role of the random

displacement. Especially simple results, coinciding with Csanady's (1963) asymptotic formulae, can be obtained from (5) in the limiting case when the terminal velocity V far exceeds typical velocities of turbulent pulsations.

In § 2 a model turbulence spectrum (Kraichnan 1970) is used to elucidate the dependence of characteristics of particle motion on the parameters defining the anisotropy due to the deterministic drift. Equation (5) is reduced to the simplest form and then integrated numerically via a procedure similar to the one used earlier in I. Asymptotic considerations for arbitrary spectra are presented in § 3, where lower and upper bounds for the particle diffusivity corresponding to a solution of (5) are derived by considering appropriate approximations for the velocity correlation equations. In § 4 we use this asymptotic approach to analyse the experimental data of Snyder & Lumley (1971). A remarkable agreement between the theory and experiment is obtained after introducing adequate corrections for the non-stationary experimental conditions.

2. A particle in turbulence with a model spectrum

Consider a turbulent field with Kraichnan's (1970) model spectrum

$$\Phi_{ij}(\mathbf{k}, t) = \frac{E(k)}{4\pi k^2} \left(\delta_{ij} - \frac{k_i k_j}{k^2} \right) \exp \left[-\frac{1}{2}(u_0 kt)^2 \right], \tag{6}$$

$$E(k) = 16(2/\pi)^{\frac{1}{2}} u_0^2 k^4 k_0^{-5} \exp(-2k^2/k_0^2), \tag{7}$$

where $k = (\mathbf{k} \cdot \mathbf{k})^{\frac{1}{2}}$ and u_0 is the typical turbulent velocity. The damping factor in Φ_{ij} is generally unknown. We have chosen here to relate the decay time of each component of the turbulence spectra to its respective wavenumber k (Saffman 1963; Weinstock 1978) rather than to use the commonly adopted arbitrary constant decay rate k_0 – hence the exponential factor in (6).

For a particle suspended in isotropic turbulence yet having a non-zero steady deterministic velocity component due to an external force, the system retains axial symmetry. The use of (6) and (7) allows the integration with respect to k in (5) to be carried out. If p_i is a unit vector parallel to the axis of symmetry, the tensorial equations for the displacement reduce to

$$\left. \begin{aligned} \frac{d^2 R_{ii}}{dt^2} &= 4\pi\gamma \int_{-\infty}^{\infty} e^{-\gamma|t-t'|} dt' \int_0^{\infty} k^2 \Phi_{ii}(k, t') dk \int_0^1 \cos(Vkt'x) \\ &\quad \times \exp \left\{ -\frac{k^2}{2} \left[\frac{3}{2}(1-x^2) R_{ii}(t') - \frac{1}{2}(1-3x^2) p_i p_j R_{ij}(t') \right] \right\} dx, \\ p_i p_j \frac{d^2 R_{ij}}{dt^2} &= 2\pi\gamma \int_{-\infty}^{\infty} e^{-\gamma|t-t'|} dt' \int_0^{\infty} k^2 \Phi_{ij}(k, t') dk \int_0^1 (1-x^2) \cos(Vkt'x) \\ &\quad \times \exp \left\{ -\frac{k^2}{2} \left[\frac{3}{2}(1-x^2) R_{ii}(t') - \frac{1}{2}(1-3x^2) p_i p_j R_{ij}(t') \right] \right\} dx, \end{aligned} \right\} \tag{8}$$

with

$$x = k_i p_i / k.$$

It is convenient to use the following variables and parameters:

$$y = k_0^2 R_{ii}, \quad y_3 = k_0^2 p_i p_j R_{ij}, \quad \tau = u_0 k_0 t, \quad \lambda = \gamma / u_0 k_0, \quad \beta = \frac{u_0}{V}, \quad \mu = \lambda \beta.$$

The first three are simply the displacement and time in a suitable non-dimensional form. λ is the ratio of turbulence to particle time constants indicating the relative importance of inertia, while β and μ are parameters associated with the anisotropy of the system. The ratio of the turbulent velocity to the deterministic part of the particle velocity, β , indicates the significance of the viscous forces relative to the body forces acting on the particle. The parameter μ is independent of the turbulent velocity and has the meaning of a reciprocal Grashoff number typical for the particle–fluid system.

With the above non-dimensional variables and parameters the relations (8) can be integrated to give

$$\left. \begin{aligned} \frac{d^2 y_3}{d\tau^2} &= \lambda \int_{-\infty}^{\infty} e^{-\lambda|\tau-\tau'|} \frac{\exp\left(-\frac{(\tau'/\beta)^2}{8(1+\frac{1}{4}\tau'^2+\frac{1}{4}y_3)}\right)}{(1+\frac{1}{4}\tau'^2+\frac{1}{4}y_3)^{\frac{1}{2}}(1+\frac{1}{4}\tau'+\frac{1}{4}y_1)^2} d\tau', \\ \frac{d^2 y}{d\tau^2} &= 2\frac{d^2 y_3}{d\tau^2} + \lambda \int_{-\infty}^{\infty} e^{-\lambda|\tau-\tau'|} \left(1 - \frac{(\tau'/\beta)^2}{4(1+\frac{1}{4}\tau'^2+\frac{1}{4}y_3)}\right) \frac{\exp\left(-\frac{(\tau'/\beta)^2}{8(1+\frac{1}{4}\tau'^2+\frac{1}{4}y_3)}\right)}{(1+\frac{1}{4}\tau'^2+\frac{1}{4}y_3)^{\frac{3}{2}}(1+\frac{1}{4}\tau'+\frac{1}{4}y_1)} d\tau', \end{aligned} \right\} (9)$$

where $2y_1 = y - y_3$. Note that although the procedure is similar to that used when studying the isotropic case in I, (9) do not reduce exactly to the equations used there in the limit $\beta \rightarrow \infty$ since the chosen damping factor is different. In the other asymptotic case when the deterministic drift far exceeds the characteristic velocity of turbulent pulsations and $\beta \rightarrow 0$, the random displacement in the exponents of (5) as well as the damping factor in Φ_{ij} can be neglected. This case will be discussed in detail in the next section for general three-dimensional spectra. With Kraichnan's model spectrum the relations (8) integrate asymptotically to give the particle velocity correlation functions as

$$\left. \begin{aligned} \frac{d^2 y_3}{d\theta^2} &= 2\mu \sqrt{\frac{\pi}{2}} e^{2\mu^2} \{e^{-\mu\theta} [1 - \operatorname{sgn}(\mu - \frac{1}{4}\theta) \operatorname{erf}(\sqrt{2}|\mu - \frac{1}{4}\theta|)] + e^{\mu\theta} [1 - \operatorname{erf}(\sqrt{2}(\mu + \frac{1}{4}\theta))]\}, \\ \frac{d^2 y}{d\theta^2} &= 2(1 - 2\mu^2) \frac{d^2 y_3}{d\theta^2} + 8\mu^2 e^{-\frac{1}{2}\theta^2}, \end{aligned} \right\} (10)$$

where $\theta = \tau/\beta = V k_0 t$.

The most interesting feature emerging from the solution of (9) and (10) is the appearance of negative transverse particle velocity correlations. The reason for their existence is that Eulerian fluid velocity correlations are negative over certain regions of time in order to satisfy continuity (Hinze 1959). An example of such behaviour, compared with the corresponding longitudinal particle velocity correlation functions, is shown in figure 1. In general, as well as in the asymptotic case, *the correlations are not self-similar*. Negative transverse correlations cannot appear if the integrand corresponding to $d^2 y_1/d\tau^2$ in (9) is positive at all times, i.e. if

$$(1 + \frac{1}{4}\tau^2 + \frac{1}{4}y_3) + \left(1 - \frac{(\tau/\beta)^2}{4(1 + \frac{1}{4}\tau^2 + \frac{1}{4}y_3)}\right) (1 + \frac{1}{4}\tau^2 + \frac{1}{4}y_1) > 0. \quad (11)$$

Since $y_1 < y_3$ while both are $O(\tau)$ at large times it is evident that the correlations are definitely positive if $\beta > 1/\sqrt{2}$ for all values of μ . When $\beta \rightarrow 0$ we deduce, with reference to (10), that negative correlations are nonetheless prohibited when $\mu < \frac{1}{2}$.

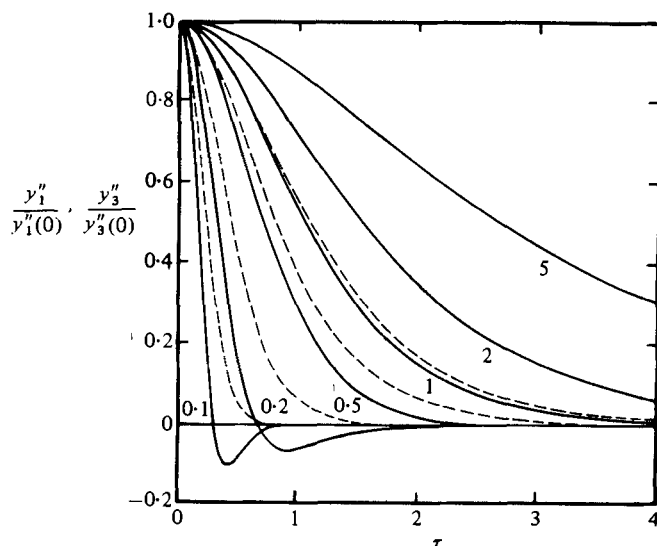


FIGURE 1. Normalized particle velocity correlation function (Kraichnan spectrum, $\mu = 2$). Numbers indicate values of β . Solid and dashed curves correspond to transverse and longitudinal correlations respectively.

Figure 2 illustrates a typical dependence of the diffusivity tensor

$$\bar{D}_{ij} = \frac{k_0}{u_0} D_{ij} = \frac{k_0}{2u_0} \lim_{t \rightarrow \infty} \frac{dR_{ij}}{dt} \quad (12)$$

on the parameters governing the anisotropy of the system, β and μ . In the region $\beta > O(1)$ the decline of the components of the diffusivity tensor is mainly due to increasing inertia and thus resembles the pattern reported in I for the isotropic case. Evidently the ratio of the longitudinal to transverse diffusivity remains near unity. When $\beta \lesssim O(1)$ the effect of the constant drift becomes significant. The deterministic velocity component, \mathbf{V} , draws the particle out of the strongly correlated fluid element, thereby reducing the diffusivity markedly, while the ratio of the diffusion coefficients sharply increases towards its ultimate value of 2 at $\beta = 0$. If the typical turbulent velocity is fixed as a certain fraction of the particle's deterministic velocity, the diffusivity exhibits only a slight dependence on the particle time constant and increases mildly with decreasing inertia as is expected.

A comparison with the results of Reeks (1977) is also incorporated in figure 2. His data appear consistently lower than our curves and the difference should be attributed mainly to the choice of the damping factors associated with the turbulence spectra. As the diffusion process is primarily determined by the long-wave modes ($k < k_0$), our particular choice for the decay factor results in larger diffusivities.

The random part of the total kinetic energy per unit particle mass

$$\bar{T} = u_0^2 T = \frac{1}{2} u_0^2 \frac{d^2 R_{ii}(0)}{dt^2} \quad (13)$$

is depicted in figure 3 for the same choice of the physical parameters. The energies of both longitudinal and transversal motion, T_3 and T_1 , are shown. Note that the limit $\beta = 0$ ($\lambda \rightarrow \infty$ at fixed μ) does not correspond to the case of non-inertial particles in a

completely isotropic system and the total energy is less than the maximum value $T = \frac{3}{2}u_0^2$ associated with the ambient turbulence. When a finite deterministic drift is present, the condition indicating the approach to this asymptotic value is $\mu \gg 1$, rather than $\lambda \gg 1$ as reported for the isotropic case. T_1 is always considerably higher than $\frac{1}{2}T_3$ and, since the particle diffusivity is proportional to the product of the integral time scale and energy, the difference between the longitudinal and transverse diffusivities must be partly attributed to a higher longitudinal integral time.

Finally, the dissipation per unit particle mass due to the random part of the motion, viz.

$$\bar{Q} = \frac{Q}{u_0^3 k_0} = -\frac{1}{2u_0^3 k_0 \gamma} \frac{d^4 R_{ii}(0)}{dt^4} = (\frac{3}{2} - \bar{T}) \lambda, \quad (14)$$

can also be evaluated from (9). Q passes through a maximum with increasing particle inertia, as in the case of no deterministic motion described in I.

3. Asymptotic considerations for general spectra

As was mentioned in the previous section, when $u_0 \ll V$ the exponents containing the random displacement in (5), as well as the damping factor in $\Phi_{ij}(\mathbf{k}, t)$, can be neglected. The fluid correlations are approximated by the Eulerian velocity correlations along the deterministic particle drift.

Evidently the Gaussian property and Corrsin's conjecture need not be employed in this case. The exceptionally simple asymptotic form of the tensorial equation (5),

$$\frac{d^2 R_{ij}}{dt^2} = \gamma \int_{-\infty}^{\infty} e^{-\gamma|t-t'|} dt' \int_{-\infty}^{\infty} \cos(\mathbf{V} \cdot \mathbf{k}t') \Phi_{ij}(\mathbf{k}) d^3 \mathbf{k}, \quad (15)$$

enables a straightforward integration. Thus, for any three-dimensional energy spectrum $E(k)$ with the normalization condition

$$\int_0^{\infty} E(k) dk = \frac{3}{2} u_0^2 \quad (16)$$

and the Eulerian length scale

$$L = \frac{\pi}{2u_0^2} \int_0^{\infty} \frac{E(k)}{k} dk, \quad (17)$$

the asymptotic form of the diffusivity tensor becomes

$$D_{ij} = \frac{Lu_0^2}{V} (\delta_{ij} + p_i p_j) = \frac{\pi}{2} \frac{u_0}{k_0} \beta (\delta_{ij} + p_i p_j). \quad (18)$$

(18) is a rederivation of Csanady's (1963) asymptotic formulae and is valid regardless of the particle inertia or relationship between the Eulerian and Lagrangian turbulent velocity correlations. The next approximation, with the damping factor in $\Phi_{ij}(\mathbf{k}, t)$ still neglected, is

$$D_{ij} = \frac{\pi}{2} \frac{u_0}{k_0} \beta [(1 + \beta^2) \delta_{ij} + (1 - 2\beta^2) p_i p_j + O(\beta^4)], \quad (19)$$

and it still asymptotically coincides with Csanady's formula for the longitudinal diffusivity, namely

$$D_{ij} p_i p_j = \frac{Lu_0^2}{V} \left(1 + \frac{u_0^2}{r^2 V^2}\right)^{-\frac{1}{2}}, \quad (20)$$

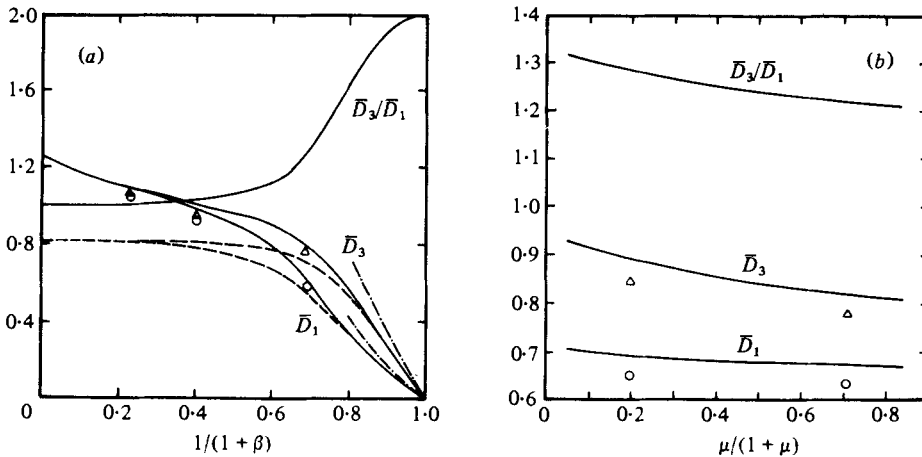


FIGURE 2. Transverse (\bar{D}_1) and longitudinal (\bar{D}_3) particle diffusivities (Kraichnan spectrum). (a) $\mu = 2$, —, exact; \cdots , equation (15); $---$, equation (21), (b) $\beta = \frac{1}{2}$. \circ and \triangle correspond to Reeks' results for \bar{D}_1 and \bar{D}_3 respectively.

when $r = 1/\sqrt{2}$. Such a comparison is no longer possible for higher-order terms in the expansion (19) since, by virtue of the original equation (15), they include integrals of the type $\int k^n E(k) dk$ ($n \geq 1$) and hence depend on details of the spectrum which do not enter into Csanady's formulae.

It is clear that the use of (15) as an approximation to (9) results in an over-estimation of the characteristic diffusion coefficient expected from a solution of (5). Such an upper bound calculated from (19) is shown in figure 2(a) for the region $\beta \ll 1$.

Another bound for diffusivity can be obtained by replacing $R_{ij}(t)$ on the right-hand side of (5) by its long-time asymptote

$$R_{ij}(t) = 2D_{ij}t. \tag{21}$$

This approximation is an appealing alternative to omitting the exponent in (5) altogether, and yields the 'self-consistent' tensorial equation

$$D_{ij} = \frac{1}{2}\gamma \int_0^\infty dt \int_{-\infty}^\infty e^{-\gamma|t-t'|} dt' \int_{-\infty}^\infty \cos(\mathbf{k} \cdot \mathbf{V}t') \Phi_{ij}(\mathbf{k}, t') \exp[-t' \mathbf{k} \mathbf{k} : \mathbf{D}] d^3\mathbf{k} \tag{22}$$

for the diffusivity tensor.

The self-consistent character of (22) suggests possible application of this equation far from the asymptotic region. Indeed, Salu & Montgomery (1977) applied this approach to the isotropic problem of turbulent self-diffusion ($\mathbf{V} = 0, \gamma \rightarrow \infty, D_{ij} = D\delta_{ij}$), obtaining the expression

$$D = \int_0^\infty dt \int_0^\infty 2\pi k^2 \Phi_{ii}(k, t) e^{-k^2 Dt} dk, \tag{23}$$

which, upon neglect of the damping factor in $\Phi_{ii}(k, t)$ and integration, yields

$$D = (\int k^{-2} E(k) dk)^{\frac{1}{2}}. \tag{24}$$

It should be pointed out that, since $Dt > \frac{1}{2}R_{ii}(t)$, (23) always underestimates the value of the diffusivity. Furthermore, returning to (22) with finite γ and integrating over t gives

$$\lim_{t \rightarrow \infty} D_{ij} = \int_0^\infty dt' \int_{-\infty}^\infty \cos(\mathbf{V} \cdot \mathbf{k}t') \Phi_{ij}(\mathbf{k}) \exp[-t' \mathbf{k} \mathbf{k} : \mathbf{D}] d^3\mathbf{k}, \tag{25}$$

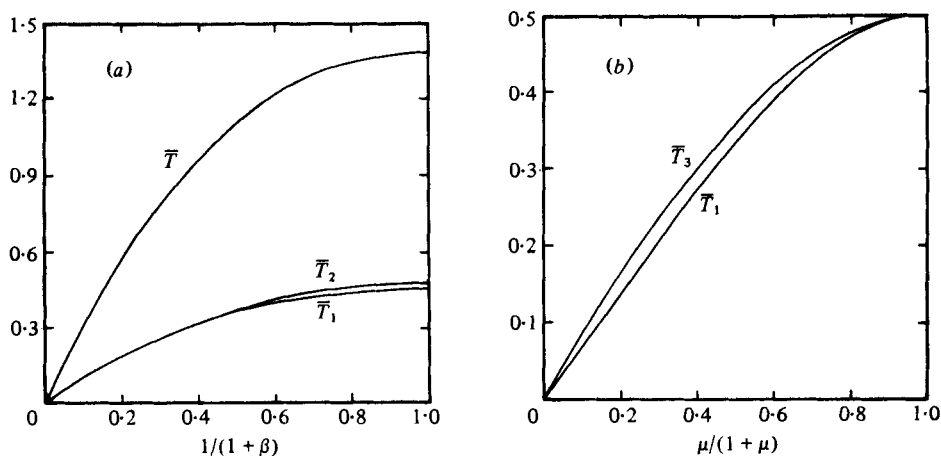


FIGURE 3. Kinetic energy of the particle random motion (Kraichnan spectrum).
(a) $\mu = 2$, (b) $\beta = \frac{1}{2}$.

a result independent of γ , the inertia parameter! The exact values, although varying rather mildly with μ for fixed β (see figure 2b), are independent of inertia only at $\beta \rightarrow 0$. Thus, the error increases with increasing inertia effects.

Figure 2(a) shows the diffusivities evaluated from the self-consistent equation (25) as lower bounds to the exact solution of (5) when Φ_{ij} corresponds to Kraichnan's model. As expected, the approximation holds over the entire range of β and improves considerably as β diminishes.

4. Analysis of the experiment of Snyder & Lumley

The most comprehensive data on particle dispersion in turbulence are those reported by Snyder & Lumley (1971). Measurements of the characteristics of the supporting turbulent field were incorporated, thereby laying the basis for a comparison with theoretical results.

The first step in the analysis of the experiments involves modification of the reported turbulent energy spectrum. The latter lacks information on its long-wave part, which is known to influence strongly the particle dispersion. Furthermore, only the transverse spectrum, $E_1(k)$, was reported, rather than the three-dimensional spectrum $E(k)$ needed for a comparison with the theory. These two obstacles are overcome by assuming that $E(k)$ is of the von Kármán-Pao form

$$E(k\eta) = a_1(k\eta)^4 [1 + a_2(k\eta)^2]^{-1/2} \exp\{-a_3(k\eta)^{\frac{1}{2}}\} \quad (26)$$

suggested by Helland, Van Atta & Stegen (1977), where a_1 , a_2 , a_3 are empirical constants and $\eta = (\nu^3/\epsilon)^{\frac{1}{2}}$, ν is the fluid kinematic viscosity and ϵ is the turbulent energy dissipation per unit mass. The spectrum (26) is proportional to k^4 for small k and exhibits a Kolmogorov-type decay, $k^{-\frac{5}{3}}$, for large k or an exponential cut-off at the dissipation-scale wavenumbers ($k\eta \sim O(1)$), depending on the particular case. Helland *et al.* (1977) have tested (26) successfully by fitting the data obtained in two inde-

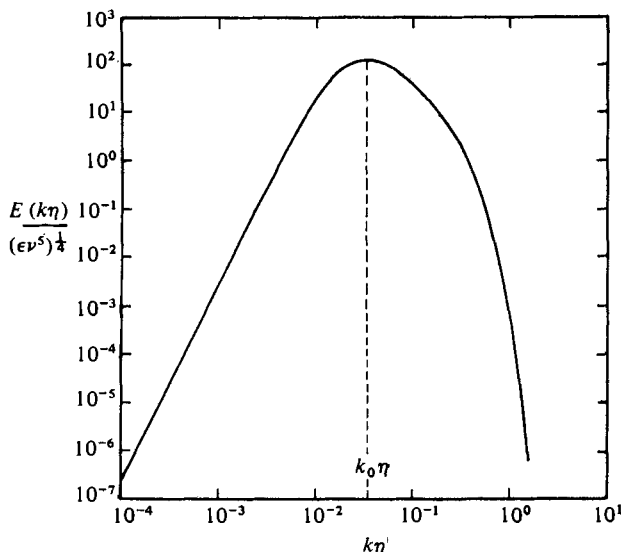


FIGURE 4. Three-dimensional normalized turbulence energy spectrum for Snyder & Lumley's experiment.

pendent grid turbulence experiments. The data of Snyder & Lumley were extrapolated by integrating (26) (Hinze 1959),

$$E_1(k\eta) = \frac{1}{2} \int_{k\eta}^{\infty} \frac{E(\xi)}{\xi} \left(1 + \left(\frac{k\eta}{\xi} \right)^2 \right) d\xi, \tag{27}$$

and choosing the constants a_1 , a_2 and a_3 to minimize the mean-square deviation from the normalized experimental transverse spectrum. The three-dimensional spectrum is depicted in figure 4.

A major disadvantage of the turbulent field described by Snyder & Lumley is the large-scale non-homogeneity along the testing channel, which is translated into a non-stationarity of the turbulence along a particle trajectory. There existed a considerable decay of the intensity with distance, typical for grid-produced turbulence in wind tunnels. Nevertheless, the spectral distribution of the ambient energy appeared from the experimental data to be self-similar. Thus, approaching the problem of turbulent decay along the particle trajectory on the basis of quasi-stationarity appears unavoidable. Such an approach is valid only if the particle time constant, characterizing the time scale during which a particle attains equilibrium with the surrounding local fluid, is sufficiently smaller than the representative decay time of the turbulent intensity. The decay time perceived by a particle suspended in the upward flow with a linear velocity U can be estimated as

$$t_r^{-1} = (U - V) \frac{d \ln u_0}{d\xi}, \tag{28}$$

where ξ is a co-ordinate along the flow. The lowest values for the experimental conditions are $t_r \approx 0.3$ s. All particle time constants, however, are still an order of magnitude smaller (see γ^{-1} in table 1). Thus, a quasi-stationarity assumption along a particle trajectory is justified.

Distance from the grid, in mesh lengths ...	Copper particles ($\gamma = 20.4 \text{ s}^{-1}$)			Corn pollen particles ($\gamma = 50 \text{ s}^{-1}$)		
	41	73	171	41	73	171
$\lambda = \gamma/u_0 k_0$	0.94	2.09	5.17	2.31	5.13	12.7
$\beta^{-1} = V/u_0$	2.46	3.69	5.67	1.01	1.51	2.33
$\mu = \gamma/Vk_0$	0.38	0.57	0.91	2.28	3.40	5.45

k_0 corresponds to the maximum of the three-dimensional spectrum in figure 4. u_0 is the characteristic turbulent velocity, as given by Snyder & Lumley.

TABLE 1. Particle parameters for the experiments of Snyder & Lumley (1971).

The next step, in view of the above distinction between the long and short time scales, is to examine particle velocity correlations at various positions along the testing channel. The most accurate approach would be to use (26) in the general tensorial equations (5), a route which would result in a formidable numerical integration procedure. Indeed, such an involved procedure could be most beneficial, had the exact functional form of the spectral decay with time been known. However, an introduction of such uncertainty implies incorporation of an adjustable parameter and would render the test of the quasi-stationarity hypothesis impossible. This can be avoided by noticing that the heavier particles in Snyder & Lumley's experiments fall roughly into the asymptotic region $u_0 \ll V$ (see table 1). Thus, it is possible to use the asymptotic expression (15) developed in § 3 for the case $\beta \ll 1$. After necessary rearrangements and changing to Snyder & Lumley's variables we arrive at the equations describing the local particle velocity correlations:

$$\left. \begin{aligned} \frac{d^2 y_3}{dt^2} &= \int_0^\infty \frac{2F_0(\gamma\eta)^2 E(k\eta)}{\eta(k\eta)^3 V^3} \int_0^{k\eta V} \frac{(k\eta V)^2 - (z\eta)^2}{(\gamma\eta)^2 + (z\eta)^2} \cos(tz) d(z\eta) d(k\eta), \\ \frac{d^2 y}{dt^2} &= \int_0^\infty \frac{4F_0(\gamma\eta)^2 E(k\eta)}{\eta(k\eta) V} \int_0^{k\eta V} \frac{\cos(tz)}{(\gamma\eta)^2 + (z\eta)^2} d(z\eta) d(k\eta), \end{aligned} \right\} \quad (29)$$

where t is a time variable within the local (short) time scale, and $F_0 = (e\nu^5)^{\frac{1}{2}}$, V and η vary only on the long time scale associated with the turbulence decay.

When applying equations (29) to Snyder & Lumley's data it is implicitly assumed that the motion of the particles follows a linear drag law. In fact the Reynolds numbers of all particles are $O(1)$ when based on their terminal velocities in air but smaller than unity when calculated using the strongest turbulent velocity fluctuation. Thus, as indicated by Lumley (1976), a linearization of the drag law with respect to the random part of the relative velocity, with a tensorial drag coefficient, is appropriate. We have further ignored the slight anisotropy introduced by the linearization and have used the experimental scalar drag coefficient reported by Snyder & Lumley.

Correlations for copper particles evaluated using (29) at different positions along the testing channel are shown in figure 5. In § 2 we have shown, for the ideal model, that particle correlation functions are not necessarily self-similar when the effect of a steady drift cannot be ignored, and that correlations may become negative depending on the particular values of the parameter μ and β . Indeed, the plot indicates a considerable reshaping of the curves with the decaying turbulence while μ and β^{-1}

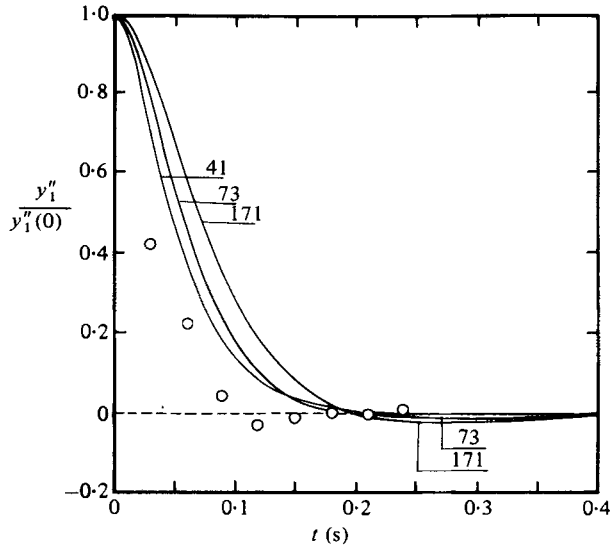


FIGURE 5. Asymptotic transverse particle velocity correlation functions for copper particles. Numbers indicate distance from the grid measured in mesh lengths. Dots correspond to Snyder & Lumley's corrected function.

increase more than twofold. (See table 1.) Note that the negative correlations appear only at the downflow positions, in consistency with the estimates in § 2, and that this results in reduction of the diffusion coefficient additional to the effect of the decay of turbulent intensity. Snyder and Lumley measured in their experiment particle displacements and average velocities between adjacent sampling stations. From these they calculated, for each kind of particle, a single correlation curve, by continuously rescaling the time axis with allowance for the turbulent decay. Thus, this corrected function implies the incorrect assumption that particle motion decays in the same manner as turbulence, retaining self-similarity. Of course, their correlation function should not correspond to any of the locally evaluated correlations since each of the latter is plotted against unscaled time but is normalized with a different kinetic energy corresponding to position along the testing channel. This is also demonstrated for copper particles in figure 5.

Before turning to large time scale integration, it should prove interesting to integrate equations (29) once locally, thereby obtaining the local particle diffusivities. In figure 6 based on the asymptotic calculations we show the variation of the transverse diffusivity along the particle trajectory for copper and corn pollen particles. Note that the diffusion coefficients exhibit a maximum at an early stage, corresponding to the inflection in the particle trajectory data, and then decay slowly with the decaying intensity of the turbulent field.

The mean squared transverse particle displacement R_{11} is calculated by integrating the quasi-stationary correlation function

$$R_{11}(t) = \int_0^t ds \int_0^s \frac{\partial^2 R_{11}(s, t')}{\partial t'^2} dt' \tag{30}$$

using properly interpolated correlation functions, each being a function of the short-scale time, at different positions depending on the particle residence time $s = \xi / (U - V)$.

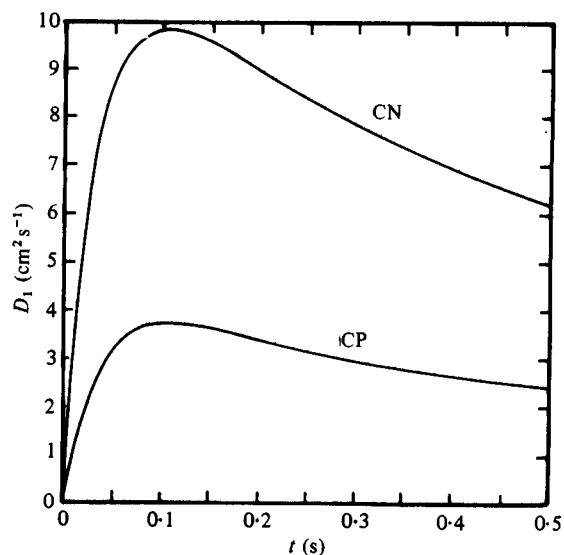


FIGURE 6. Variation of the local transverse diffusion coefficients for copper (CP) and corn pollen (CN) particles.

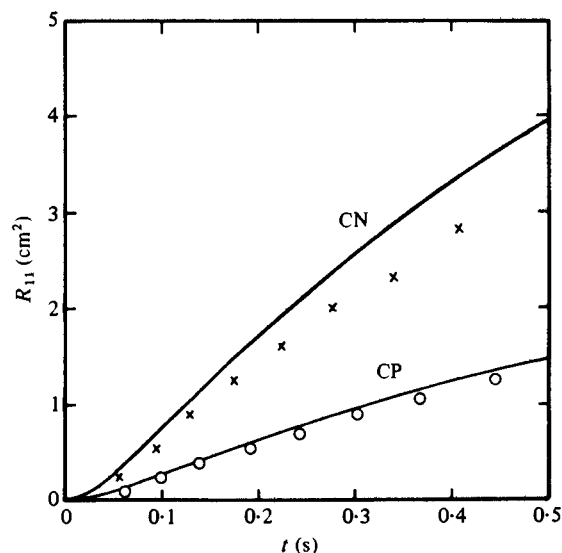


FIGURE 7. Mean-squared transverse particle displacement. Snyder & Lumley's measurements for copper (O) and corn pollen (x) particles and asymptotically evaluated curves.

Figure 7 shows the resulting integrated curves. For the heavy copper particles, where the assumption that β lies in the asymptotic region is completely justified, the agreement with the experiment is excellent. As the deviation from the asymptotic region increases, the calculations tend to over-estimate the actual diffusivities, as is evident for the corn pollen. The correct shape of the curve is preserved nonetheless. It should be stressed here that this remarkable agreement between the theory and the experiment is obtained without any semi-empirical or other adjustable parameters, and confirms the quasi-stationarity of the dispersion process.

The authors are grateful to H. Horn for his help in the APL programming.

REFERENCES

- CORRSIN, S. 1959 *Adv. in Geophysics* **6**, 161–184.
CSANADY, G. T. 1963 *J. Atmos. Sci.* **20**, 201–208.
HELLAND, K. N., VAN ATTA, C. W. & STEGEN, G. R. 1977 *J. Fluid Mech.* **79**, 337–359.
HINZE, J. O. 1959 *Turbulence*. McGraw-Hill.
KRAICHNAN, R. H. 1970 *Phys. Fluids* **13**, 22–31.
LUMLEY, J. L. 1976 *Topics in Appl. Phys.* **12**, 289–324.
LUNDGREN, T. S. & POINTIN, Y. B. 1976 *Phys. Fluids* **19**, 355–358.
PHYTHIAN, R. 1975 *J. Fluid Mech.* **67**, 145–153.
PISMEN, L. M. & NIR, A. 1978 *J. Fluid Mech.* **84**, 193–206.
REEKS, M. 1977 *J. Fluid Mech.* **83**, 529–546.
SAFFMAN, P. G. 1963 *Appl. Sci. Res. A* **11**, 245–255.
SALU, Y. & MONTGOMERY, D. 1977 *Phys. Fluids* **20**, 1–3.
SNYDER, W. H. & LUMLEY, J. L. 1971 *J. Fluid Mech.* **48**, 41–71.
WEINSTOCK, J. 1978 *Phys. Fluids* **21**, 887–890.
YUDINE, M. I. 1959 *Adv. in Geophysics* **6**, 185–191.